The International Journal of Indian Psychology
ISSN 2348-5396 (e) | ISSN: 2349-3429 (p)
Volume 7, Issue 4, DIP: 18.01.056/20190704
DOI: 10.25215/0704.056
http://www.ijip.in | October- December, 2019

Research Paper

A mathematical model of the Gunas as a foundation for expanded understanding of decision-making process

Mauricio Garrido[1], David Wolf[2]*

ABSTRACT

Based on empirical validation (Stempel (2006); Wolf (1999)) of the constructs of the three gunas, as described in the Vedic literatures, a mathematical model depicting the mechanism of action of the gunas was developed. This model was evaluated using data from a group design study on the effects of maha mantra meditation. Analysis demonstrated substantive validity for this mathematical model of the three gunas, or modes of material nature- sattva (enlightenment), rajas (activity), and tamas (inertia). On the foundation of this mathematical modeling, guna theory was applied to approaches to decision-making, and specifically to the leaky competing accumulator (LCA) model. Guna theory enriches the LCA, and decision-making theory in general, by combining an accumulation model with personality traits and providing enhanced understanding of the effects of environmental factors on the process of decision-making.

Keywords: *Gunas, Decision-Making, Mantra Meditation, Maha Mantra, LCA Decision-Making Model, Leaky Competing Accumulator*

Vedic literatures present the three *gunas* as both the very substance of both matter and the filters through which we perceive the world. Research related to the development of the Vedic Personality Inventory (VPI) has indicated strong validity and reliability for the constructs of the three *gunas*, as described in ancient Vedic literature (Stempel, et al., 2006; Wolf, 1999, 1998). The lead author of this study developed a mathematical model depicting the mechanism of how the *gunas* operate, individually and interactively. Data from studies on the *Maha mantra* (Wolf and Abell, 2003) was used to test this model, and the results indicate robust validity for this mathematical understanding of the *gunas*. This article reports on application of the *guna* paradigm to decision-making theory and process, and suggests potentially vital conceptual and practical applications for utilizing the guna model in decision-making processes.

[1]Ph.D., physicist, research associate with the Bhaktivedanta Institute for Higher Studies, United States of America (USA)
[2]Ph.D. and supervisor of psychotherapists, Satvatove Institute, Florida, United States of America (USA)
*Responding Author
Received: November 9, 2019; Revision Received: December 17, 2019; Accepted: December 25, 2019

Mathematical Model of the Gunas

We begin by creating a 3D state-space with the three *gunas* as axes, each with a scale of 0-100% (Fig 1).

Figure 1: Guna State-space. Each axis is one of the gunas (sattva, rajas, and tamas) with a scale of 0 -100%. Thus, every point on the 2D triangle shown represents a mixture of the gunas adding up to 100%.

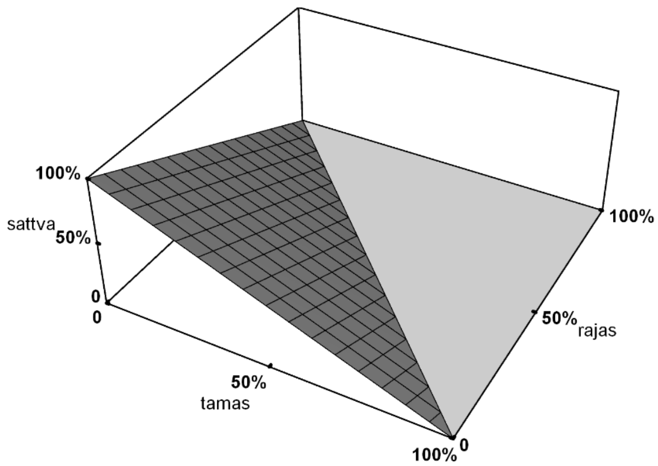

In order for these percentage numbers to be meaningful, we impose the condition that the sum of the coordinates of a specific point be 100%. This allows us to intuitively think of an object, or the state of a person, as a composition of the three *gunas*. It also reflects the competition for dominance among the *gunas*: as one coordinate increases, the others will necessarily decrease. This condition also confines our space to a 2D triangle, so it makes sense to take the coordinate axes to be the triangle's 2D coordinates, which are best expressed by barycentric coordinates λ_{sattva}, λ_{rajas}, and λ_{tamas} (Fig 2) with the condition

$$\lambda_{sattva} + \lambda_{rajas} + \lambda_{tamas} = 100\%$$

Figure 2: Barycentric coordinates on the guna-space triangle. The different coordinates are zero along different edges of the triangle and increment along the dashed lines to a maximum at the corners. Sattva is at a maximum of 100% at the top corner and 0% along the bottom edge, rajas is max at the bottom right corner and min at the left edge, and tamas is max at the bottom left corner and min at the right edge.

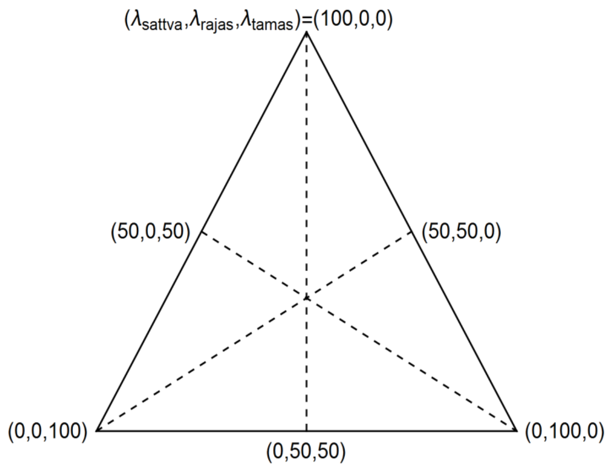

The self-state of a person is represented by a point on the triangle. Objects and situations that affect the self are represented by points called attractors, which pull on the self with a force which we model to include three main characteristics:

1. The direction of the force in *guna*-space.
2. The force being inversely proportional to the distance (the farther away the attractor is from the self-state in *guna*-space, the weaker the force the attractor will exert).
3. The specific strength of an attractor. Even if two different attractors are at the same distance from the self-state, one may attract more due to its nature. E.g. a food attractor may exert a stronger pull on a person than a music attractor, even if they're both at the same distance.

The total force is the sum of all the attractor forces and it follows a Newtonian-like law-

$$F = \sum_{i=1}^{N} \frac{s_i(\vec{x}_{self} - \vec{x}^i{}_{attractor})}{\left\|\vec{x}_{self} - \vec{x}^i{}_{attractor}\right\|^2} = Ia$$

where N is the total number of attractors, $\vec{x}_{self}$ is the position vector of the self, $\vec{x}^i{}_{attractor}$ that of the i-th attractor, s_i the specific strength of the i-th attractor, I an inertial "mass" tensor of the self-state that resists change, and a the acceleration produced in the *guna*-space (see Fig 3).

Figure 3: Attractors. In the figure below, the self-state is represented by a square. The two points at the end of the arrows represent attractors (objects or situations one experiences) that pull on the self-state with different force strengths and directions. The forces pulling on the square are represented by arrows F1 and F2. They can be time-dependent or independent. For plotting ease, the coordinate axes are the triangle's x-y coordinates. The corners of the triangle are the points where a guna is at 100%.

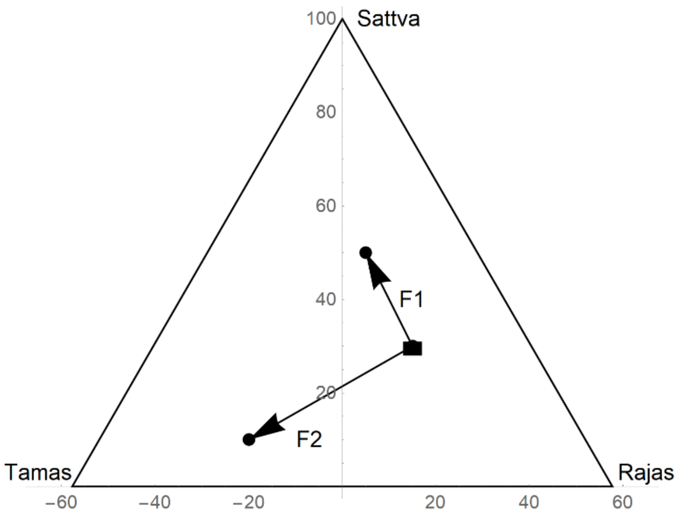

The inertial mass tensor I informs us how easy it is for the self to move in a particular direction. The most general expression of the inertial mass tensor is

$$I = \begin{pmatrix} I_{sattva-sattva} & I_{sattva-rajas} & I_{sattva-tamas} \\ I_{rajas-sattva} & I_{rajas-rajas} & I_{rajas-tamas} \\ I_{tamas-sattva} & I_{tamas-rajas} & I_{tamas-tamas} \end{pmatrix}$$

With this, we can calculate how the component of the force in one direction is affecting the motion in another direction. Example: $F_{sattva} = I_{sattva-rajas} a_{rajas}$ tells us how the component of a force in the *sattva* direction is affecting the motion in the *rajas* direction. The utility of having such a matrix for the inertial mass, as opposed to a single mass number, is that we can now talk about how a person can have proclivities to move more easily in a certain direction than another due to past conditionings. For example, a person with a problem of drug addiction, may be more prone to move more easily in the *tamas* direction than in the other two directions.

In barycentric coordinates, we can diagonalize the matrix to find a simplified form

$$I = \begin{pmatrix} I_{sattva} & 0 & 0 \\ 0 & I_{rajas} & 0 \\ 0 & 0 & I_{tamas} \end{pmatrix}$$

where I_{guna} is the component of the inertial mass tensor along the direction specified by the *guna; i.e. sattva, rajas or tamas*. An idea for obtaining these three parameters empirically, as well as the position vector of the self, will be discussed in the next section (section 4).

Monte Carlo Simulation of Maha Mantra Meditation Experiment

In order to test our model, we need a dynamic experiment in which the *gunas* have been quantified. Wolf and Abell (2003) carried out just such an experiment to determine the effects of meditation. They measured the *gunas*, stress, and depression with statistically-validated Likert-type tests before the intervention, after 28 days of meditating, and again 28 days after the last day of the intervention. The test to quantify the *gunas* —the Vedic Personality Inventory, or VPI—was previously developed and validated by Wolf (1999) and later generalized and further validated by Stempel, et al. (2006). It consists of a series of 56 Likert-type questions, each having a score ranging from 1 to 7. How the coordinates for the self-state in the *guna* space were obtained from this test is described in the Appendix.

Please note, Wolf and Abell mentioned in their paper (2003) that, as expected from *guna* theory, there was significant increase in *sattva* and decrease in *tamas*, stress, and depression between pretest and posttest; and also as expected, the opposite occurred between posttest and followup. Surprisingly however, *rajas* had no significant change throughout the experiment. This will be important when we contrast the simulation results and these experimental results later in this article.

To model the effect of the *mantra* meditation, we note that due to the fact that *mantra* meditation is traditionally practiced to obtain clear perception, we have taken it to be a fully *sattvic* activity, so it was modeled as a strong attractor with 100% *sattva*.

Besides the *mantra* attractor, it is safe to say that the participants of the study were also experiencing many other forces in their lives at the time of the study. Since we do not know the specifics of those other forces, we can at least create a situation in our simulation that will lead our simulated self-state to have the same average position in *guna*-space as the mean average pretest position of the participants. To this end, four equidistant attractors of equal force magnitude were placed surrounding the initial self-state to keep it in its place. These were placed above, below, and on the sides of the initial self-state, each at a distance equal to the standard deviation of the pretest.

We should clarify that the values for the mean average and standard deviations were taken from the pretest for the *mantra*-chanting group specifically from this study (presented again in Table A-1) and converted to barycentric coordinates, as detailed in Appendix A, because it's the group that showed a significant dynamical change in their state due to the meditation attractor. To make this arrangement more realistic and to ensure that the self-state is brought back to the original position (on average) if it wanders away from the center, a Monte-Carlo simulation was designed by temporarily increasing the force magnitude of different attractors randomly several times during the simulation. This accounts for the random and temporary nature of our encounter with different attractors throughout our day (Fig 4).

Monte-Carlo simulations introduce a random variable in a simulation to obtain numerical results. They are most useful when it is difficult or impossible to use other approaches, including modeling phenomena with significant uncertainty in inputs, such as the calculation of risk in business or our current model.

Figure 4: Simulation set up for the meditation experiment. Four equidistant attractors of equal force magnitude (round points) surround the self-state (solid square) and are randomly and temporarily boosted in a Monte-Carlo simulation.

This is meant to simulate the subject's average attractor forces. The time-dependent attractor for the meditation technique is 100% *sattva*, so it is placed at the top. It's active only during the first half of the simulation time. The circle at the top highlights the position of this *mantra* meditation attractor. The dashed square maps the simulation region shown in Fig 5.

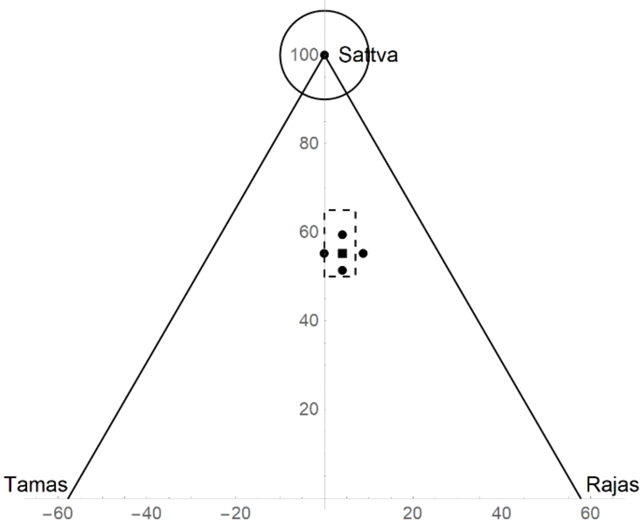

The simulation time was divided into two equal parts, with the meditation attractor active only during the first half.

RESULTS AND ANALYSIS

The model successfully reproduced the results of the Wolf & Abell (2003) experiment in the vertical direction, showing an increase towards *sattva* during the pretest to posttest period, and a decrease between posttest and followup (Fig 5).

Figure 5: Mean ±SD from the pretest, posttest and followup of the meditation experiment.

The triangle's x-y coordinates correspond to the simulation region marked by the dashed square in Figure 4. The inset arrows point to the barycentric coordinate directions for reference.

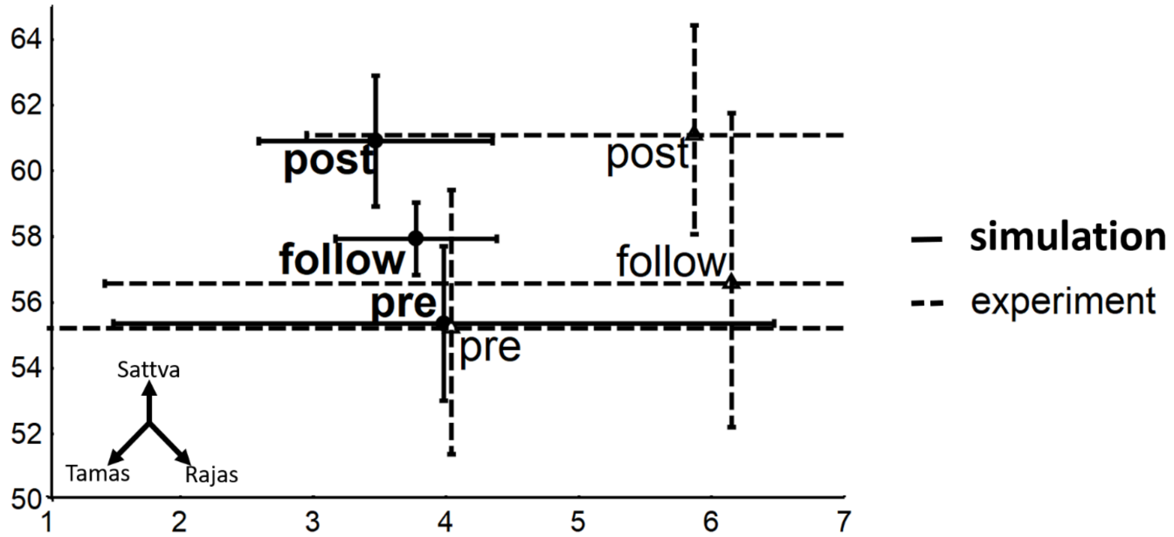

When the parameters were set up to create pretest and posttest vertical mean values of the simulation to match the experiment, a followup mean value of the simulation was obtained that is a modest 1.46 standard deviations higher than the followup experiment. We can decrease that followup mean value little by little, by further tweaking different parameters, such as the attractor force magnitudes and simulation time. However, this tweaking also has the unwanted effect of increasing the size of other standard deviations, as well as the sensitivity to initial conditions, due to increasing the effect of random forces throughout the simulation.

In the horizontal direction, or x-axis, on the other hand, there is a qualitative difference that persisted throughout the simulation runs. The mean value of the posttest simulation is always to the left of the pretest simulation, while the mean value of the posttest experiment is on the other side (to the right of the pretest experiment). As mentioned previously, this is the surprising result that the *rajas* did not change as expected. We will calculate this below.

The horizontal mean value of the posttest experiment is within a less moderate 2.51 standard deviations to the right of the horizontal mean value of posttest simulation; and in the case of the followup, the horizontal experimental mean reaches a significant 3.79 standard deviations to the right of the horizontal simulation mean.

To understand this difference in the results, let us look at Fig 4 again. We must take into account the fact that the attractor for the meditation technique is situated at the top of the triangle on the vertical axis, which is also to the left of the simulation area shown (green rectangle).

Thus, it will always pull any self-state in that area (which is magnified in Fig 5) towards the upper left, making the simulation posttest invariably lean towards the left of the simulation pretest.

This upper-left leaning is actually the qualitative result (a notable decrease in *rajas*) Wolf and Abell were expecting from *guna* theory when they performed their experiment (2003) on chanting the *hare krsna maha mantra*, as mentioned in the previous section. To see it, take the barycentric coordinates of the simulation pretest and posttest. We went from a simulation pretest mean score $\lambda_{pretest}^{simulation} = (55.37, 25.98, 18.65)$ to a simulation posttest mean score $\lambda_{posttest}^{simulation} = (60.90, 22.58, 16.52)$. Leaning towards the upper left direction therefore corresponds to an appreciable decrease in *rajas* of $\Delta_{rajas} = 25.98 - 22.58 = 3.40$. That is a 13.09% decrease from the pretest. On the other hand, the experiment went from $\lambda_{pretest}^{experiment} = (55.22, 25.89, 18.89)$ to $\lambda_{posttest}^{experiment} = (61.09, 24.54, 14.37)$, which yields a decrease in *rajas* of only $\Delta_{rajas} = 1.35$. A 5.21% decrease from the pretest. Therefore, our model is recreating the expected results from *guna*-theory and the experiment, except in regards to the *rajas* component for the experiment.

To visualize this better, let us look at the equipotentials of Figure 6. The dashed lines represent all the points that have the same value for *rajas* in the barycentric coordinates and have thus been labeled. In figure 7, we see how the simulation posttest has a significant higher *rajas* than the simulation pretest. On the other hand, figure 8 shows us that the experimental posttest did not differ that much from the experimental pretest. Figure 9 shows both the experimental and simulation differences.

Figure 6. Equipotentials. In barycentric coordinates, the points having the same value of rajas are located along diagonal lines.

The X and Y coordinates have also been plotted to allow easy identification of the region being described in other graphs where a close up is taken.

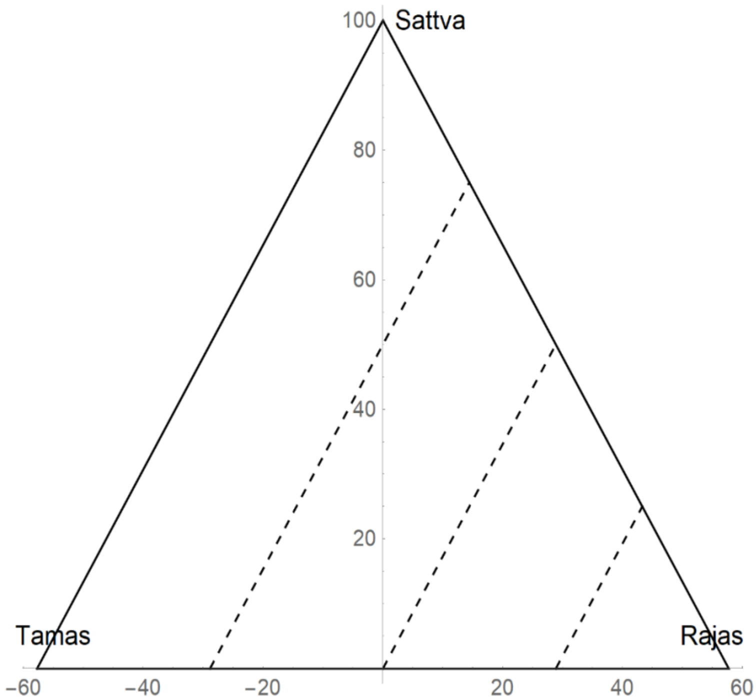

Figure 7. Difference in rajas values in the simulation.
The simulation pretest and posttest differ in their *rajas* values by 3.40. Equipotentials for the raja values of the simulation pretest and posttest have been added for a better visualization of this.

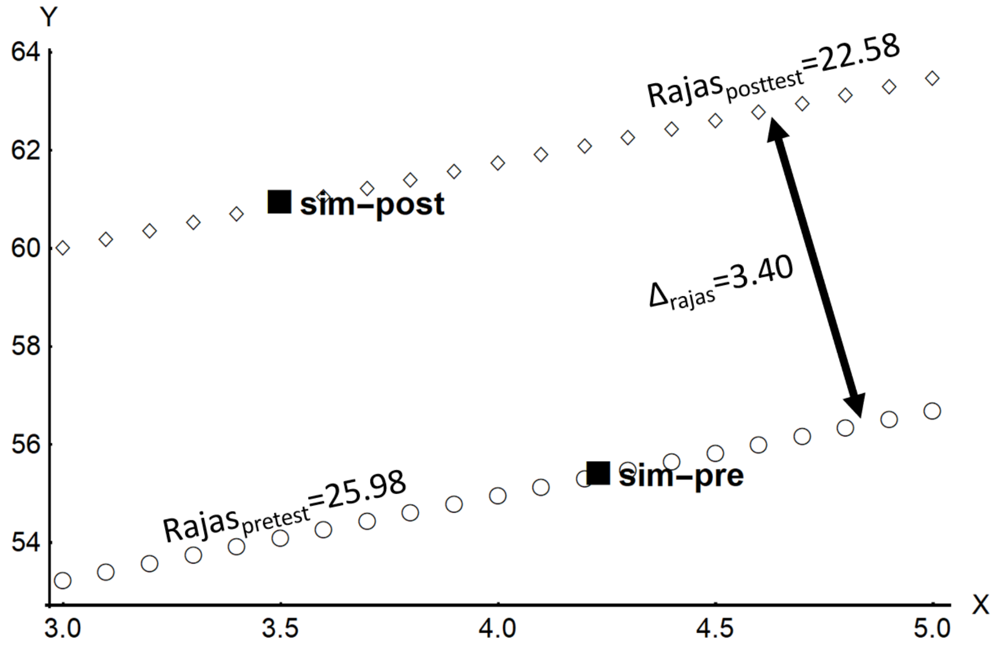

Figure 8. Difference in rajas values in the experiment.
The experiment pretest and posttest differ in their *rajas* values by 1.35. Equipotentials for the raja values of the simulation pretest and posttest have been added for a better visualization of this.

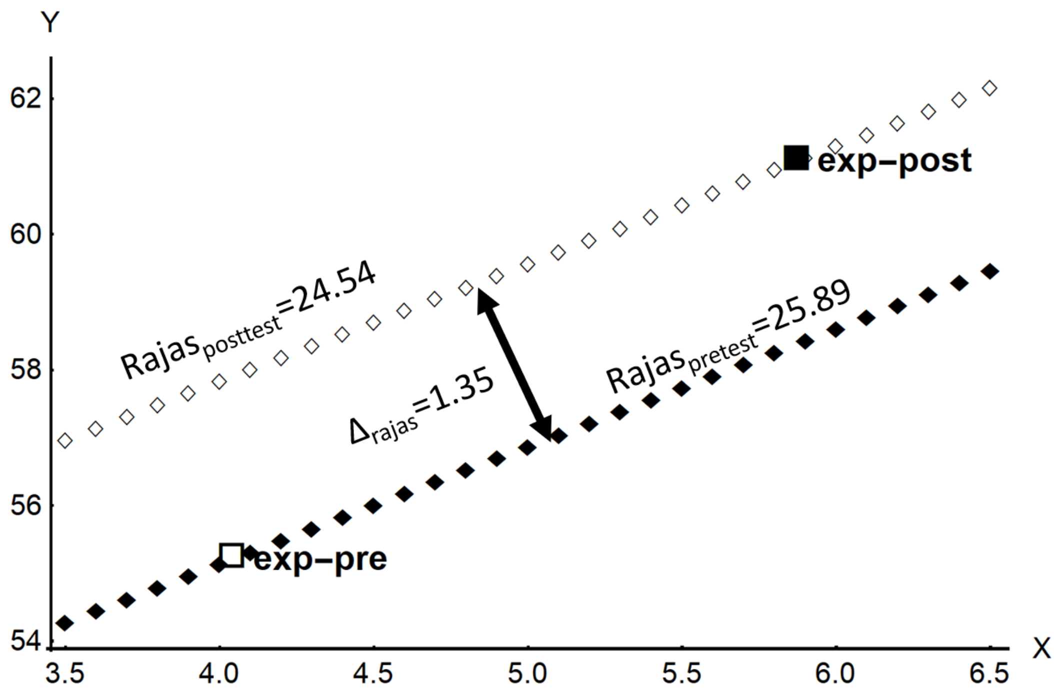

Figure 9. Comparison of the difference in rajas values for the experiment and the simulation.

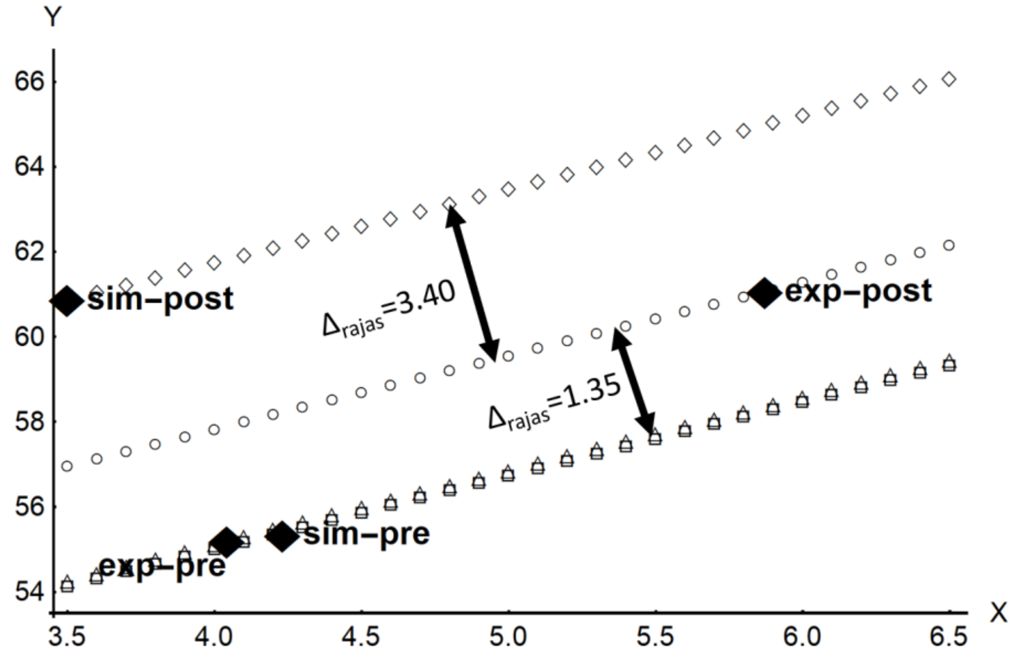

Wolf and Abell postulated a possible explanation for the lack of change in the *rajas* component of the experiment in their article in Research on Social Work Practice (Wolf and Abell, 2003):

"An explanation for the nonsignificant *rajas* results is also found in the Vedas, where it is described that *rajas* is an intermediate mode between *tamas* and *sattva* (Wolf, 1999). Therefore, it is conjectured that some *rajas* transformed into *sattva*, as predicted by Vedic theory, but some *tamas* transformed into *rajas*, and thus the level of *rajas* remained constant." "Statistical analysis confirms that *rajas* is an intermediate mode between *sattva* and *tamas*." (Wolf, 1999 (2))

From the point of view of *guna*-space, this suggests there may be a preferred path that the self-state may take when traveling *guna*-space. One that goes from *tamas* to *sattva*, and vice-versa, via *rajas*. This could be modelled using some sort of gradient potential. However, the treatment of this experiment in *guna*-space also suggests other possibilities that are worth exploring.

Possible reasons for having the experimental posttest and followup to the right of the experimental pretest might include:

1. There was an event in the community that created a strong *rajas* attractor (e.g. elections, exams, a series of big sports matches, etc.), which lasted at least through the 28 days from posttest to followup.

   We can check for evidence by looking at the data from the alternate *mantra* and control groups in Fig 10.

Figure 10: Mean pretest, posttest and followup scores of the mantra simulation and the three experiment groups.

The data for the control and alternate group were treated in the same fashion as the *mantra* experiment group (detailed in the appendix) to obtain the data points shown in the figure.

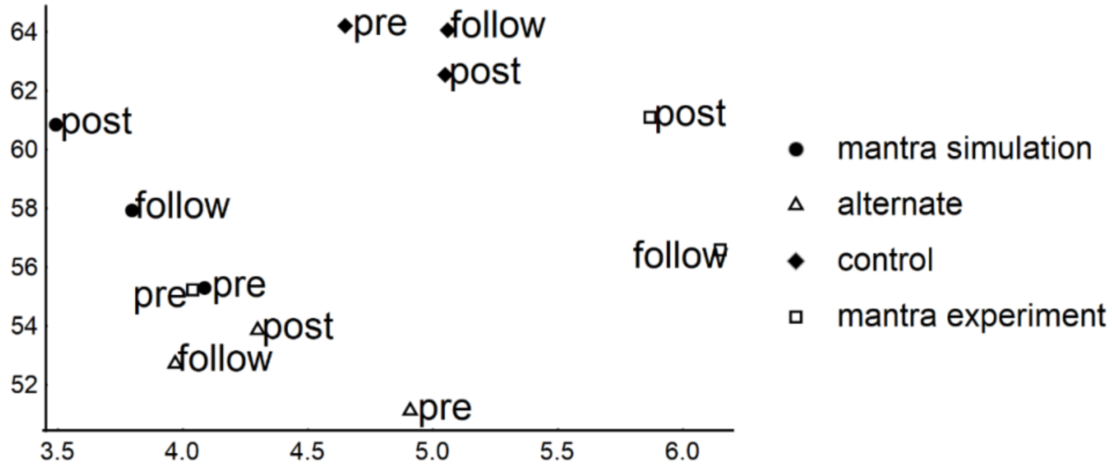

The figure shows no special correlation among the three experimental groups (*mantra* experiment, alternate *mantra* and control) that would indicate a strong *rajas* attractor in the community at that time. If there was such a strong *rajas* attractor, we would expect all three experimental groups to have their mean posttest and followup to the right and likely lower than their mean pretest. This was not the case for the alternate *mantra*. Thus, this possibility is untenable.

2. Even though the meditation attractor is 100% *sattva*, it might be offset or masked by the inexperience of the subjects. This conjecture could be tested by including seasoned practitioners in future experiments, and checking for a gradual offset with practice time.
3. The inverse subscale percentage may not be the best measure for the inertial mass. By increasing the I_{rajas} and decreasing I_{sattva} and I_{tamas}, we could better reproduce the shift of the posttest and followup towards the right of the pretest. However, there is an intuitive feeling that the inverse subscale percentage *does* convey the resistance to change in a particular direction. If someone scores high on a particular *guna*, that suggests they're more in tune with that *guna*. Thus, changing the definition of the inertial mass, or simply forcing it to conform to the experimental results, should be considered only after testing option 2 described above.

OVERVIEW OF DECISION-MAKING MODELS

As an application of tri-*guna* theory to decision theory, we've enhanced an existing well-known mathematical model of decision-making to include the effects of a decision maker's surroundings on his/her choice.

Decision theory is divided into different branches, depending on the goal of the analysis: normative or prescriptive, and descriptive. Normative decision-making tries to identify the best decision based on a set of uncertain beliefs and a set of values, and assumes a fully rational decision maker who can compute with perfect accuracy. It tells us how we ought to make decisions. Some common models of this type are expected utility theory and Bayesian probability revision.

Descriptive decision-making, on the other hand, as the name suggests, describes the way in which decisions are actually taken, which can significantly deviate from the prescriptive models, as in the case of risky choice situations. Thus, rather than being grounded in a set of axioms, as in the normative case, the models are developed from cognitive process theories. Two known models of this type are decision field theory and the leaky competitive accumulator model. (Busemeyer et al., 2015).

The Leaky Competitive Accumulator (LCA) Model

The leaky competitive accumulator (LCA) model was developed almost two decades ago by Usher and McClelland (2001 and 2004) as an alternative to the decision field theory (DFT). Like the DFT, the LCA model is a dynamical stochastic model that assumes that perceptual choices and response times are due to the accrual of evidence. Because of this, it alludes to a neural plausibility, where it is conceivable that electrical potentials in certain neurons accumulate over time until a threshold is reached, that has made it grow in popularity over the years.

The idea behind the LCA model is that during the course of making a decision, the decision maker switches attention between different attributes or events related to the choices. This dynamic process of deliberation gives rise to a sequential sampling process according to which the subjective values of the consequences are compared and accumulated sequentially over time until either:

1. The accumulation process for one of the choices reaches a preset threshold, or
2. A preset time is reached.

When one of these two conditions are met, a decision is taken. For the first condition, the decision corresponds to the choice whose accumulation process first reaches the threshold. For the second condition, the decision corresponds to the choice whose accumulation process is biggest at the preset time. See Figure 11.

The LCA model also includes Tversky and Kahneman's (1991) loss aversion curve to account for a person's perception of losses and disadvantages having a greater impact on preferences than gains and advantages.

This model is good for evaluating multi-alternative choice problems and has been shown (Pleskac et al. 2015) to address context effects among other factors.

Figure 11. Evaluation of three choices in the LCA model with a preset threshold.

As a dynamic stochastic process, the LCA model compares different choices (indicated by the numbers 1, 2, and 3 in the graph) by updating the preference state of each, which is an accumulation process *A(t)*. When one of the accumulation processes reaches a preset threshold, the choice whose accumulation process reached it first is selected. In the graph below, it was choice number 1.

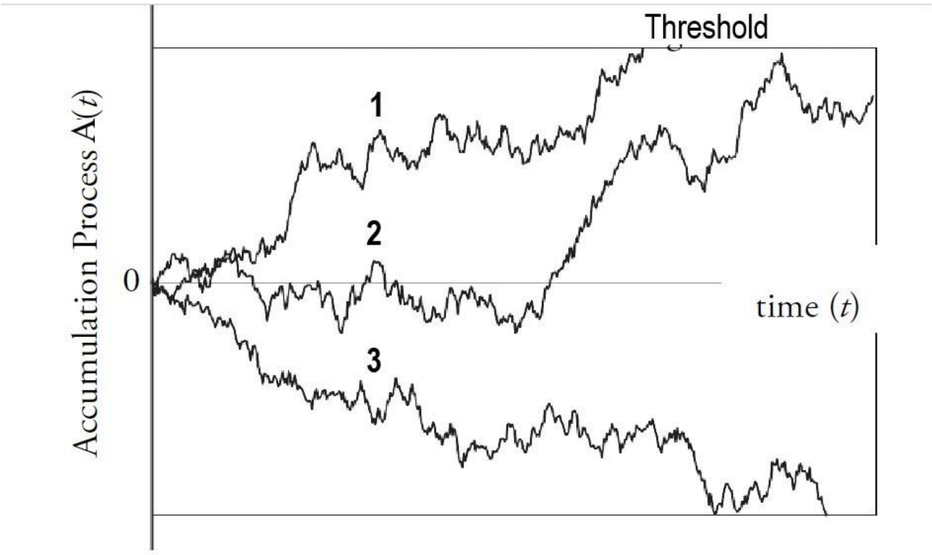

However, the current LCA model (and DFT as well) mainly deals with the choice maker and the choice problem itself. It does not take into consideration how the surroundings of the choice maker affect his/her choice.

Guna-enhanced LCA (GLCA)

It is well known that our surroundings affect our choices: going without the usual morning coffee, a rainy day, a beautiful girl selling some product, casino tactics, hearing some distressing news about something personal, etc., can produce substantial changes to the way we make decisions. Our environment has the potential to change our mood, our preferences, our states of mind, which reflects in the way we approach choices. Advertising companies have been perfecting this art for many years, and yet, mathematical models of decision-making are still lacking this effect in their analyses.

But how do we connect the myriad of phenomena that can potentially affect a decision maker with the different mind states they elicit, and furthermore, with the actual process of decision-making? For this, the language and constructs of the *gunas* are a powerful tool.

The *gunas* describe the inner mental states of a decision maker and the external phenomena affecting him/her in the same terms, viz. *sattva*, *rajas*, and *tamas*. The model we developed in a previous section tells the way in which the inner mental states of the decision maker will change by coming in contact with external stimuli. In order to include the effects of the mental states in decision-making problems, we have generalized some of the parameters found in the LCA model using tri-*guna* theory. Specifically, we have chosen four parameters to work with: threshold, neural decay constant, loss aversion curve, and attention probability weights for attributes.

In what follows, the generalization of the four mentioned parameters of the LCA model has been done taking into account the fact that a decision maker predominantly in the mode of *sattva* is logical and premeditative, while one predominantly in the mode of *rajas* tends to rush and be overwhelmed, and it will take a lot to move one predominantly in the mode of *tamas* to take a decision.

Threshold

The first parameter that we generalize is the threshold value. The mode of *rajas* will affect this value by lowering it, thus creating the sense of rushing to make a decision. The mode of *tamas*, on the other hand, will have the effect of raising the threshold value to indicate the longer period of time that it will take for a decision maker in this mode to reach a decision and/or how strong the preference must be for a specific choice to be selected.

The simplest generalization for the threshold value, then, corresponding to the ideas above would be:

$$\theta = \theta_0 + \theta_1 \times \lambda_{tamas} - \theta_2 \times \lambda_{rajas}$$

where θ_0, θ_1, and θ_2, are all positive real numbers (θ_0 being the value that would have otherwise been assigned in the LCA model), and λ_{tamas} and λ_{rajas} are the barycentric coordinates corresponding to the self-state of the decision maker as mentioned in section 3.

Figure 12. GLCA with guna-dependent threshold value.

The effect of a higher value of *tamas* is to raise the threshold, while the effect of a higher *rajas* is to lower the threshold.

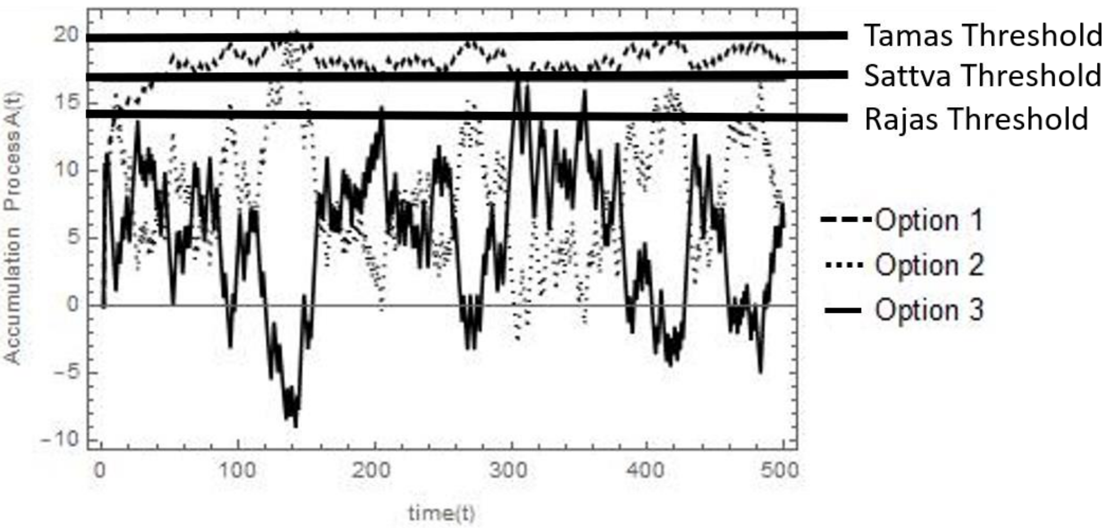

In figure 12 we see an example of a decision problem with three options. If the decision maker is predominantly in the mode of *sattva*, the first accumulation process to reach the threshold is option 1. However, if the decision maker is predominantly in the mode of *rajas*, the threshold is lower and the decision maker rushes into choosing option 3, which is the first one to reach the threshold. If the decision maker is predominantly in the mode of *tamas*, the threshold is raised so high, that none of the options reach it and thus the decision maker ends up not choosing any option at all.

Neural Decay Constant

The next parameter we generalize is the neural decay constant η (the leakage). In the accumulation formula

$$A_i(t+1) = \eta A_i(t) + (1-\eta)\left[I_i(t) - \beta \sum_{j\neq 1} A_j(t) + \xi_i(t)\right]$$

the neural decay constant η serves to account for memory and motivational processes. In some ways, it is a measure of how well a person retains previous comparisons as he/she switches back and forth between alternatives and accrues more information. The higher the neural decay constant, the faster a person reaches a decision. The neural decay constant does this by weighing the previous preference $A_i(t)$ state in the accumulation process (Pleskac et al., 2005).

This constant is generalized similar to the previous one, making both a higher degree of *rajas* or *tamas* decrease the neural decay constant

$$\eta = \eta_0 - \eta_1(\lambda_{rajas} + \lambda_{tamas})$$

where η_0, $\eta_1 > 0$. In the case that λ_{rajas} or λ_{tamas} happen to be large, then η becomes small, slowing down the accumulation process. This results in *rajas* and *tamas* driving a decision maker into a state of fluster, as seen in figure 13.

Figure 13. GLCA with guna-dependent neural decay constant.
In the top graph, the decision maker, who is in a predominantly *sattvic* self-state, as indicated on the top *guna*-space triangle on the right, has three options to choose from and quickly comes to decide for option 1, which reaches the threshold first. The middle and bottom graph show a decision maker predominantly in the mode of *rajas* and *tamas*, respectively. Because of a lower neural decay constant both graphs evidence him/her being flustered.

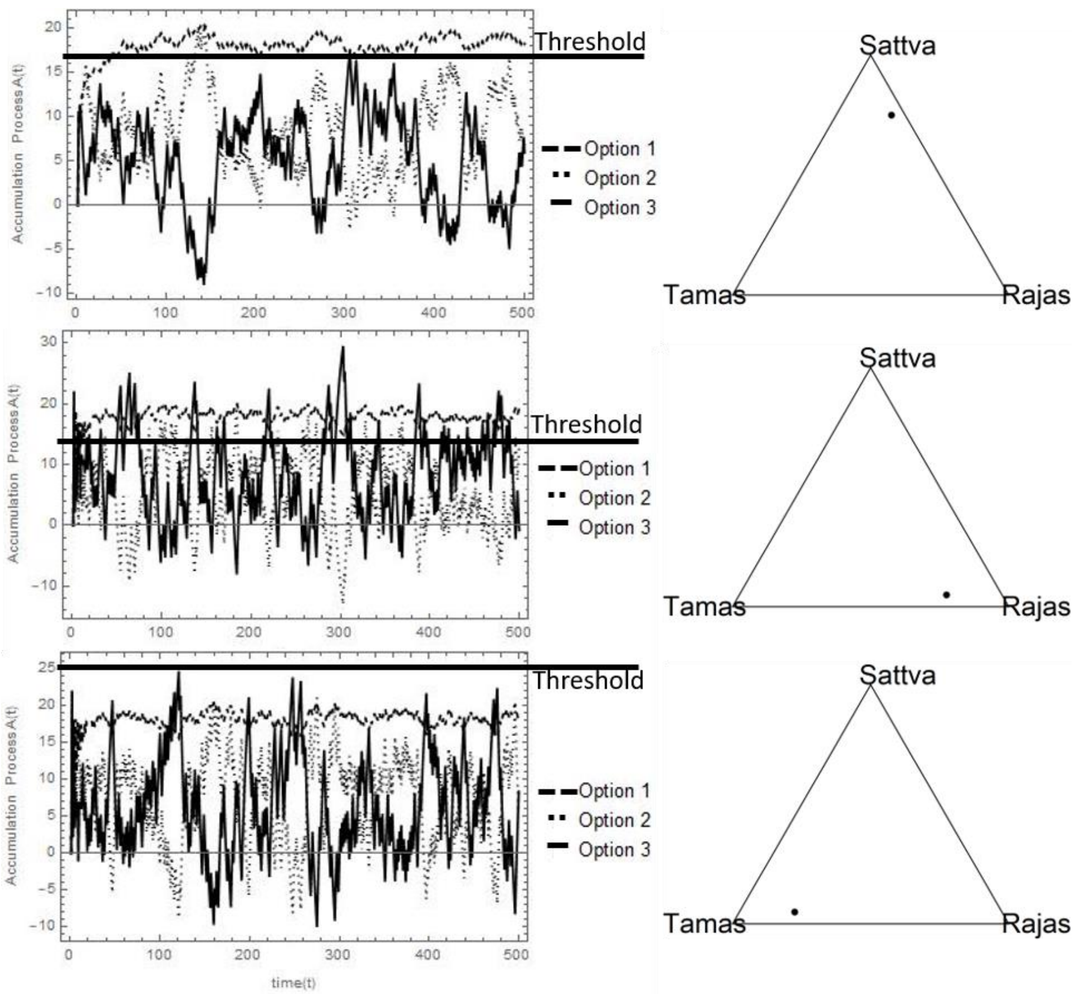

In the simulations of Figure 13, we've assumed a simple decision problem with three options. For consistency, we'll assume this same problem for the rest of the parameters we'll be generalizing. Let us imagine a decision maker who wants to buy a car and has three options. There are two attributes he's mostly interested in, viz. fuel economy and performance. He rates the three options using a scale of 0 (lowest preferable) -10 (highest preferable) and records it as in table 1.

Table 1. Preference Values for the example of buying a car. The values run from 0 (lowest preferable) -10 (highest preferable).

	Fuel Economy	**Performance**
Option 1	3	5
Option 2	4	3
Option 3	0	7

In Figure 13, top left, we see a clear and quick choice for option 1 from a decision maker predominantly in the mode of *sattva*, whose self-state is graphically represented by the point in the *guna*-space triangle on the top right. Option 1, as seen in table 1, stands as a compromise, between fuel economy and performance.

The middle and bottom graphs of figure 13, corresponding to a decision maker predominantly in the mode of *rajas* and *tamas*, respectively, show how a decrease in the neural decay constant leads to a state of fluster, i.e. option 1 no longer stands out above the other two options. For the person in the mode of *rajas*, because of a lower threshold, this means a rush to make a decision from a point of high uncertainty. A person in the mode of *tamas* is also equally flustered, but because of a higher threshold, the fluster leads him/her to give up on making a decision altogether.

Loss Aversion Curve:
The loss aversion curve proposed by the LCA

$$F(x) = \begin{cases} log(1+x), & x > 0 \\ -[log(1+|x|) + log(1+|x|)^2], & x < 0 \end{cases}$$

is consistent with Tversky and Kahneman's (1991) reference dependent model, in which losses and disadvantages have greater impact on preferences than gains and advantages. One way to generalize this curve to include the *gunas*, is suggested below-

$$F(x) = \begin{cases} log(1+x) + 2(1-\lambda_{sattva})log(1+x)^2, & x > 0 \\ -[log(1+|x|) + \lambda_{sattva}\, log(1+|x|)^2], & x < 0 \end{cases}$$

This new formula for the GLCA reduces to the LCA proposed equation, when $\lambda_{sattva} = 1$. In other words, it is consistent with the LCA for a *sattvic* decision maker, who is fully rational. As *rajas* and *tamas* are increased, the shape of the curve becomes more pronounced for positive values and less pronounced for negative values. This marks a tendency in *rajas* and *tamas* to become more risk seeking (giving higher value to gains and advantages), and less averse to loss (giving lower value to losses and disadvantages).

Figure 14. Modification of the loss aversion curve.
The top left graph, corresponding to a *sattvic* decision maker, shows a loss aversion graph on the top right similar to Tversky and Kahneman's. The solid curve is the loss aversion graph. The dashed curve is a graph of y=x for comparison. The middle left and bottom left graphs

correspond to a *rajasic* and *tamasic* decision maker, respectively. For both of these cases, the modified loss aversion curve is the solid curve on the bottom right.

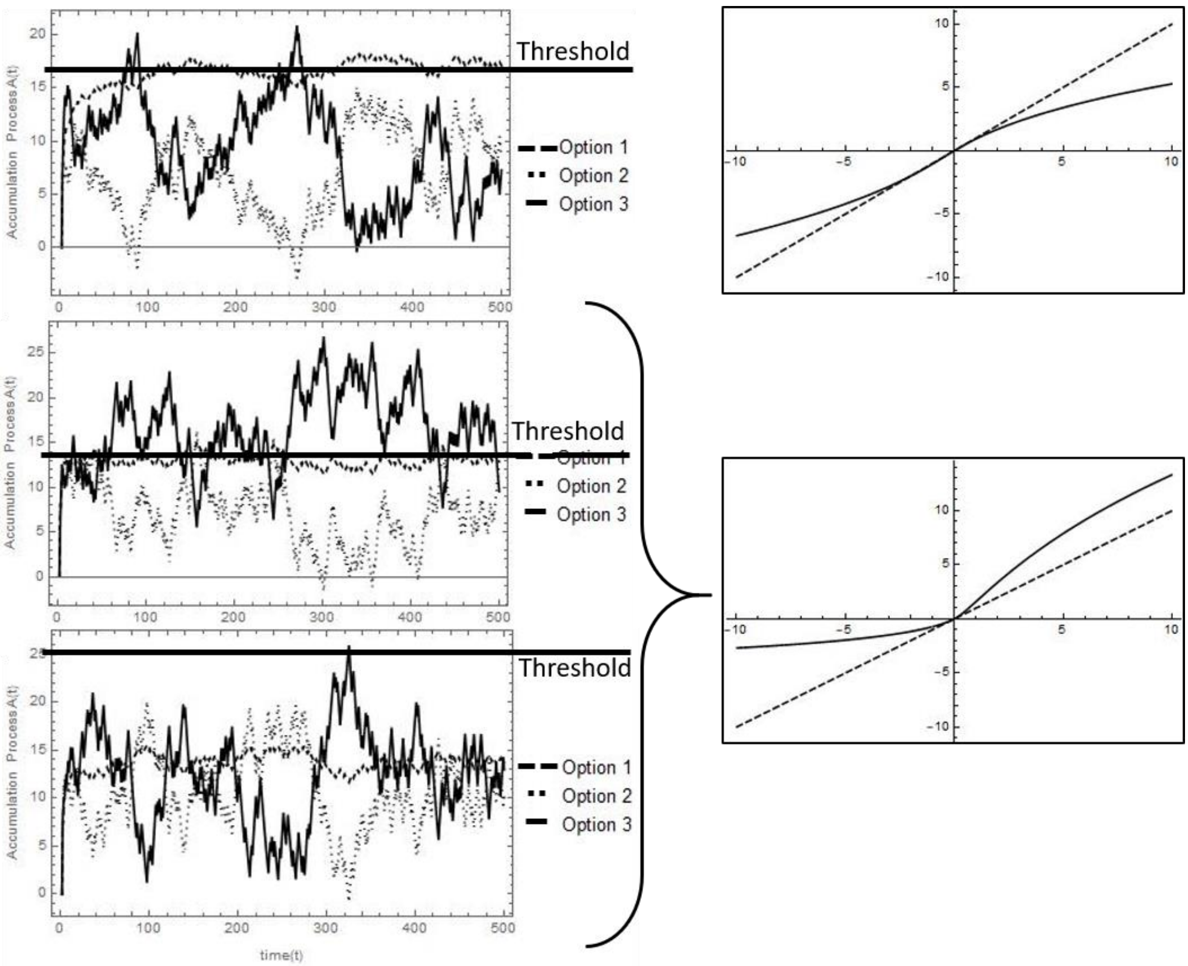

The top left graph in figure 14 corresponds to a *sattvic* decision maker. His loss aversion curve (solid curve in top right) is close to the proposed LCA loss aversion curve. In the decision problem of buying a car explained above, the *sattvic* decision maker quickly chooses option 1.

For a decision maker predominantly in the modes of *rajas* and *tamas*, the loss aversion curve (solid curve in the bottom right) has been modified strongly to show the effects more visibly. The middle left graph corresponding to a *rajasic* decision maker again shows a state of fluster and a rush to make a decision, because of the low threshold.

The bottom left graph corresponding to a *tamasic* decision maker also shows a state of fluster, but ends up choosing option 3 after some time. The option has to be so appealing, though, that it reaches the high threshold that characterizes the *tamasic* decision maker.

In both the *rajas* and *tamas* cases above, we see that option 1 does not accumulate to as high a preference state as options 2 and 3. This is because of the over-appreciation of gain and advantage from the modified loss aversion curve. Options 2 and 3 have the highest fuel economy and performance scores, respectively, and thus, whether considering one attribute or the other, the difference always leaves option 1 as much less preferable.

Attention Probability Weights for Attributes:

How much time is spent giving attention to an attribute, or equivalently, how often an attribute is chosen to be analyzed in the LCA model depends on the probability weights assigned to each attribute. We can generalize this in the GLCA when we can clearly recognize a specific *guna* at work in a certain attribute. In our previous example, we could say that the desire for prestige, which is very strong in a decision maker predominantly in the mode of *rajas* or *tamas*, is linked to the performance of the car. Therefore, we could assign probability weights such that

$$w_{economy} = \lambda_{sattva}$$
$$w_{performance} = 1 - \lambda_{sattva}$$

Figure 15. Probability Weights.

The graphs on the left are the accumulation process for a decision problem with probability weights modified as mentioned in the main text, which correspond to a decision maker predominantly in the mode of *sattva* (top), *rajas* (middle) and *tamas* (bottom), respectively. The graphs on the right indicate the self-state of the decision maker in the *guna*-space triangle with a point.

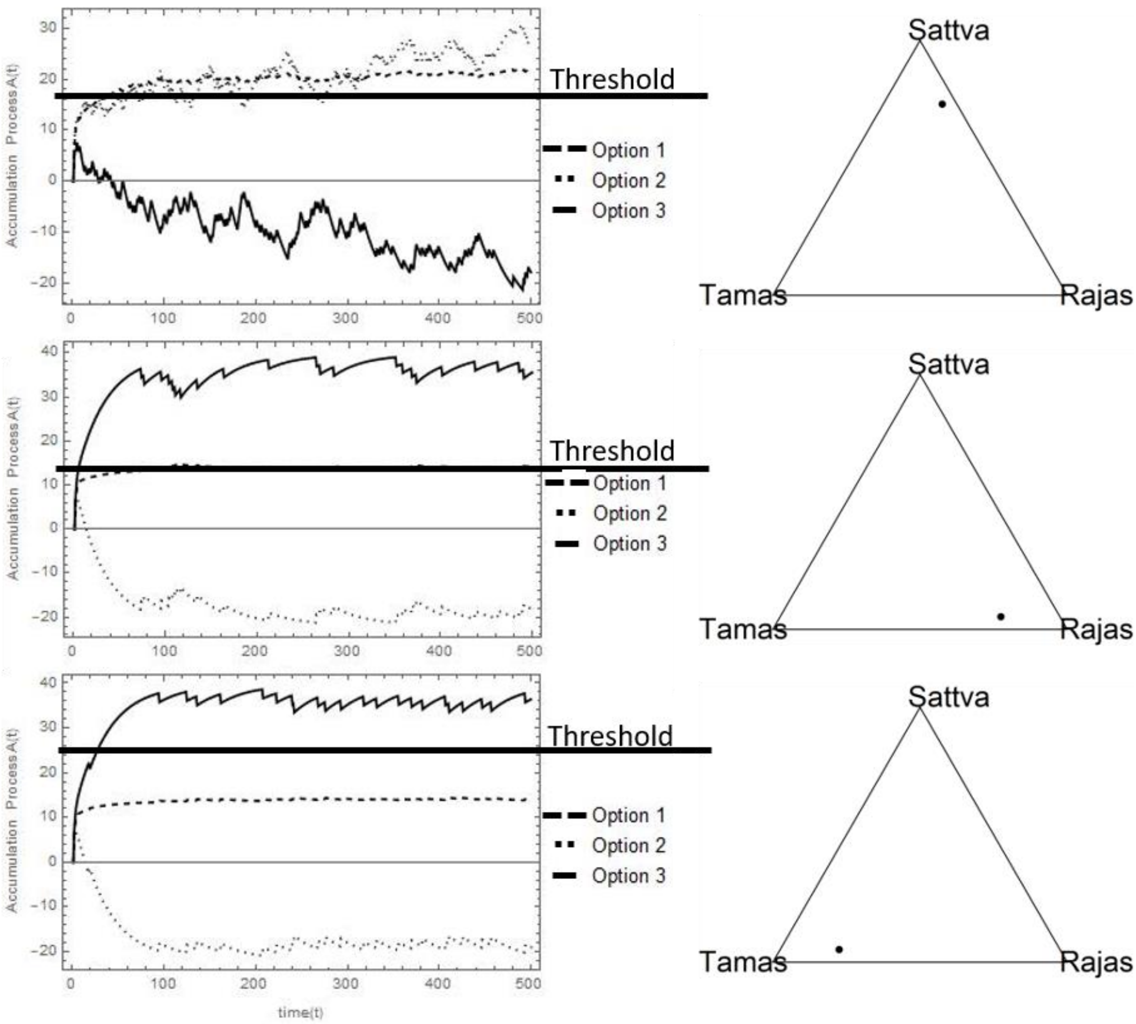

The top graph on figure 15 shows a *sattvic* decision maker, who is mainly interested in fuel economy. Thus options 1 and 2 are most preferable for him/her, while option 3 is highly discarded. Option 2 is chosen first, but is not too far away from option 1.

As *rajas* and *tamas* become more prominent, performance also becomes the prominent attribute on which the decision maker's attention is focused. Hence, option 3 takes the lead, while option 2, having the lowest performance score, is highly discarded. Option 1 is still somewhat considered, being in between, but not much. Because of the low threshold, the *rajasic* decision maker chooses option 3 quite fast and confident, while the *tamasic* decision maker, due to the higher threshold, takes longer to make the decision, but still does it, because of the high preference state for option 3.

The attributes of the options may or may not lend themselves to be easily characterized by a simple *guna* equation as in the above example. Likewise, the assumptions that have gone into the loss aversion curve, the threshold and neural decay constant modifications will require empirical testing for the whole of *guna*-space in order to strengthen the model. In any case, the fact that we now have a powerful tool to account for the way external influences impact a decision maker's choice, shows the advantage of including the tri-*guna* theory into decision making models, such as the LCA.

Empirical Evidence for the GLCA

Though direct empirical tests of the GLCA are yet to be performed, empirical evidence may nevertheless be indirectly found in the existing literature.

Recent studies by Knutson et al. (2008) have begun to show the neuropsychological mechanisms that may underlie effective emotional appeals in financial, marketing, and political domains. Although not explicitly making use of tri-*guna* theory, their results show a potential correlation between the *gunas* and neuropsychological mechanisms.

The experimental design was such that subjects would first be shown a cue, followed by one of three visual stimuli: positive (erotic pictures for 15 heterosexual men), negative (pictures of spiders and snakes), or neutral (pictures of household appliances). Then subjects would be presented the choice to make one of two preset gambles: a low-risk gamble or a high-risk gamble. Finally, the result of the gamble would be revealed.

The study showed that anticipation of viewing rewarding stimuli increased financial risk-taking. Using event-related functional magnetic resonance imaging, the effect was said to be partially mediated by increases in nucleus accumbens activation, thus concluding that even incidental reward cues may influence financial risk-taking.

From the point of view of tri-*guna* theory, the experiment is consistent with the idea that erotic pictures strongly drive a subject into the mode of *rajas*. As we have seen in the previous section, both *rajas* and *tamas* lead to a modification of the loss aversion curve that increases the appreciation for gains and advantages and decreases the aversion to losses and disadvantages, effectively making the subject more risk-taking.

Furthermore, we can see that according to tri-*guna* theory, the other two stimuli in the experiment (pictures of household appliances, and snakes and spiders) would not be expected to have as appreciable of an effect on the subjects' financial decision as the erotic pictures.

The reason being that unless a specific subject happens to have a strong repulsion or attraction for such pictures due to previous conditionings in his/her life, these categories of attractors, at least in pictures, will not generally have the strength to pull on the self-state significantly. In terms of the force equation given in section three, we may say that the specific strength s_i for the pictures of these types of things is rather low, and thus the self-state of a person will remain mostly where it is, resulting in an unaltered financial risk behavior.

Lacking the subjects' initial and final self-states from a VPI test makes it difficult to simulate this experiment, as we did for the experiment of Wolf and Abell (2003). However, it does confirm the fact that incidental reward cues, or let us say, the surroundings of a decision maker, may influence financial risk-taking, and that experimental tests on the GLCA will yield interesting results.

DISCUSSION

A mathematical model of the *gunas* has been developed, which includes an application to decision-making. This model indicates one possible way to use a powerful intuitive framework to account for interactions between a person's external surroundings and internal mental processes. The *guna*-space dynamics presented herein are simple, but they are able to reproduce both the behavior expected from tri-*guna* theory and experimental results found in the literature.

For the experiment of Knutson et al. (2008), the GLCA model, at least in principle, is able to account for the observed changes or lack thereof in financial decision making.

For the experiment of Wolf and Abell (2003), the simulations reproduced most of the results found therein. Such analysis opens up three interesting research avenues:

1. **Attractor forces for masses of people and dynamics of collective *gunas*.**
   Even though in this case, we found no evidence for a strong *rajas* attractor in the community at that time, it does suggest that a study of different attractor forces over entire communities (elections, gardening projects, natural disaster relief, new businesses, new diets, war, etc.), noting how they impact the collective self-state of the communities, could be fruitful. The study could highlight several interesting questions, such as: Under what conditions are communities better prepared for sudden change? Are there properties of the community, such as quarrelling, generosity, depression, theft, education level, etc., that form well-defined regions in *guna*-space that could exhibit critical behavior (in a statistical mechanics sense)?
2. **Time-dependent meditation effects over the years.**
   To test if the experimental discrepancy was a result of variation in the meditation experience of the participants, we could design a study to include a wide range of practitioners, spanning from rank beginner to seasoned veteran. Or perhaps do a periodic followup of the sample over several years' time, being sure to include a list of attractors to assess lifestyle changes.
3. **Redefinition of the inertial mass tensor.**
   The inverse subscale percentage may turn out to not be the best measure for the inertial mass. That would suggest a study searching for a better empirical measure of the natural resistance to change in *guna*-space.

Further directions for advances in the model include

- Determining the most influential attractors for a person or a community (environment, peers, food, books, etc.) and their ranges of specific strength.
- Evaluating the degrees to which a person can change his/her average *gunas* based on their present psychophysical nature.
- Testing the inverse proportionality between force and distance in *guna*-space for higher order powers. In the present model we assumed an inverse linear relation of $\sim \frac{1}{distance}$, but it may be the case that a better approximation might be an inverse square distance, $F \sim \frac{1}{distance^2}$, or higher.
- Developing decision-making experiments similar to that of Knutson et al. (2008), and including in them the VPI to test for transitions of self-state. Such investigations could conceivably be conducted in practically all spheres of life, since Vedic-based hypotheses regarding *guna* theory are virtually comprehensive in regards to life areas.

  For example, Gladwell (2000) describes the precipitous decline in the crime rate in New York City in the early and mid-1990s. From immersion in an epidemic of serious, felonious crime that seemed uncontrolled and unstoppable, within a very few years New York became the safest large city in the United States. For decades, conventional methods, such as increasing the police force and stiffer punishments, were ineffective in stemming the tide of the crime wave.

  What made the drastic difference is what criminologists James Q. Wilson and George Kelling call the Broken Windows theory. Though felonies were rampant, New York administrators and law enforcement authorities focused on what seemed to many to be relatively insignificant issues, and small crimes. For instance, they scrupulously cleansed the graffiti from the subway cars at the end of each day, cracked down on subway farebeating, cleared away broken glass and repaired broken windows, and rigorously attended to misdemeanors that previously were practically disregarded (Gladwell, 2000).

  Traditional explanations founded in nature-based and nurture-based social science theories fail to effectively account for the sharp reduction in crime in New York. *Guna* theory, particularly in how it relates to assessment of environmental attractors, provides a helpful framework for explaining phenomena such as the shift in crime in New York.

  The model of the three *gunas* is based on the principle of things moving from subtle, or the realm of thought or consciousness, to external manifestation. Cleanliness and orderliness are symptoms of *sattvic* consciousness (Prabhupada, 1972). As evidenced by the VPI research (Wolf, 1999), a criminal mentality and subsequent criminal actions will find it difficult to endure in a *sattvic* environment. Studies such as those conducted by Dhanaraj and Srinivasan (2019), Balaji Deekshitulu (2015), and Padam et. al. (2017) provide further evidence that sattvic practices such as mantra chanting and certain musical vibrations produce favorable effects on the mental, emotional and physical dimensions.

Studies could be constructed related to effects of environmental factors connected with decisions affecting relationships, residence, monetary considerations, diet, and practically each field of life's endeavors. In this way the GLCA could be further assessed in terms of its predictive, concurrent, and postdictive validity.

The Vedas, as confirmed by the VPI (Stempel, et al., 2006), depict *sattva guna* as a sort of empirical basis for happiness, fulfillment, security, life satisfaction, inner peace, and, generally speaking, most if not nearly all of the internal experiences that humanity tends to seek. That is, there is a clear, positive correlation between cultivation and development of *sattvic* habits and life paradigms, with those interior states of being for which people strive.

A meaning of "*guna*" is "rope", or "string". We can imagine an entangled mess of strings. Most strings we pull will harden the knot. There can be one string, though, that if pulled a certain way, will cause loosening and disentanglement. That string represents the *sattva guna*. In each circumstance, whether in the realm of financial management, emotionally-charged personal relationships, or physical health concerns, *guna* theory encourages identifying and implementing a *sattvic* choice, thus piercing the Gordian knot that muddles consciousness, and freeing the self towards full, clear and clean expression and contribution. Thus, GLCA has the potential to provide a framework for decision-making that will substantially enhance quality of life.

Vedic theory, as confirmed by VPI research, asserts, essentially, that a predominance of sattva guna correlates to enhanced capacity for making intelligent decisions that will truly serve the best interest, in the most profound sense, of the person. Srivastava, et. al. (2015) confirm that intelligence and intellect are vital factors for overall well-being and with regard to meaningful productivity.

- Correlating different neuropsychological and physiological mechanisms to the *gunas*. The recent study of Damerla, et al. (2018), on the effects of the *sattvic* practice of chanting the *hare krishna maha mantra* on heart health are a start in this research direction.
- Evaluating assumptions made for the GLCA parameter generalizations and expanding it to other parameters. One such parameter might be the initial states of the accumulators $A_i(t = 0)$, which represent previous biases and preferences, or the global inhibition parameter β, which deals with the way alternatives are compared.
- Applying tri-*guna* theory to other mathematical models of mental processes, such as addictions and phobias.

Appendix A

The VPI consists of a series of 56 Likert-type questions, each having a score ranging from 1 to 7. Because the number of questions that test each *guna* varies (15 questions for *sattva*, 19 for *rajas*, and 22 for *tamas*), the minimum score for each *guna* was subtracted from their respective raw data score. This recalibrates all three scores to a minimum of zero. Thus, for example, the recalibrated score for *sattva* would be $\lambda_{sattva}^{recalibrated} = \lambda_{sattva}^{raw\ score} - 15$.

The score for each *guna* was then divided by the maximum possible recalibrated score for that *guna* ($\lambda_{sattva}^{\text{recalibrated max } possible} = 105 - 15 = 90$ for *sattva*, 133 -19 = 114 for *rajas*, and 154 – 22 = 132 for *tamas*), giving the subscale percentage of that *guna*:

$$\lambda_{guna}^{subscale\ percentage} = \frac{\lambda_{guna}^{recalibrated}}{\lambda_{guna}^{\text{recalibrated max } possible}}$$

The sum of the three subscale percentages does not necessarily add up to 100% and thus cannot be used immediately as the coordinates of the *guna*-space. However, it does tell us what percentage of the questions for each *guna* were answered positively, and therefore can be used to measure how easily a person can move in the direction of that particular *guna*; i.e. the inverse of the component of the inertial mass:

$$I_{guna} = \frac{1}{\lambda_{guna}^{subscale\ percentage}}$$

The coordinates for the *guna*-space can be obtained by dividing the subscale percentage for each *guna* by the sum of the three subscale percentages. In this way, we impose the condition to add up to 100%:

$$\lambda_{guna} = \frac{\lambda_{guna}^{subscale\ percentage}}{\lambda_{sattva}^{subscale\ percentage} + \lambda_{rajas}^{subscale\ percentage} + \lambda_{tamas}^{subscale\ percentage}}$$

The following table lists the mean score values from the *maha mantra* chanting experiment for the group that chanted the *maha mantra*.

Table A1: Raw scores, subscale percentage and coordinates for the mean values of the experiment's pretest, posttest and followup.

Original Scores					Recalibrated Subscale %				Coordinates		
	Sattva	Rajas	Tamas		Sattva	Rajas	Tamas		Sattva	Rajas	Tamas
Pretest	70.4	51.9	49.8		61.56%	28.86%	21.06%		55.22%	25.89%	18.89%
Posttest	77.3	50.7	43.5		69.22%	27.81%	16.29%		61.09%	24.54%	14.37%
Follow up	72	53.5	46.2		63.33%	30.26%	18.33%		56.58%	27.04%	16.38%

REFERENCES

Balaji Deekshitulu P.V. (2015). Role of mantras in mental health. *International Journal of Humanities and Social Science Studies*, Vol. 1-6, 34-39. ISSN: 2349-6959 (Online), ISSN: 2349-6711.

Busemeyer, J.R., Wang, Z., Townsend, J.T., & Eidels, A. (2015). *The Oxford Handbook of Computational and Mathematical Psychology*.

Damerla, V. R., Goldstein, B., Wolf, D., Madhavan, K., and Patterson, N. (2018). Novice Meditators of an Easily Learnable Audible Mantram Sound Self-Induce an Increase in Vagal Tone During Short-term Practice: A Preliminary Study. Integrative Medicine: A Clinician's Journal. Novice Meditators of an Easily Learnable Audible Mantram Sound

Self-Induce an Increase in Vagal Tone During Short-term Practice: A Preliminary Study, Vol. 17-5, 20-28.

Dhanaraj, K., and Balaji Srinivasam, V. (2019), State anxiety and anger levels among listeners of Vedic mantra chanting. *The International Journal of Indian Psychology*, Vol. 7-1, 887-891. DIP:18.01.099/20190701, DOI:10.25215/0701.099.

Gladwell, M. (2000). *The Tipping Point*. Little, Brown and Company: Boston.

Knutson, B., Wimmer, G. E., Kuhnen, C. M. & Winkielman, P. (2008). Nucleus accumbens activation mediates the influence of reward cues on financial risk-taking. *NeuroReport*, 19, 509–513.

Padam, A., Sharma, N., Sastri, O.S.K.S., Mahajan, S., Sharma, R., and Sharma D. (2017). Effect of listening to Vedic chants and Indian classical instrumental music on patients undergoing upper gastrointestinal endoscopy: A randomized control trial. *Indian Journal of Psychiatry*, 59-2, 214-218.

Pleskac, T.J., Diederich, A., & Wallsten, T.S. (2015). Models of Decision Making Under Risk and Uncertainty. *The Oxford Handbook of Computational and Mathematical Psychology*. p225. New York: Oxford University Press.

Prabhupada, A. C. B. S. (1972). *Bhagavad-gita As It Is*. Collier Books and Macmillan Company: New York.

Srivastava, S., Goyal, P., Tiwari, S. K., Patel, A. K., and Singh, A. (2015). Intelligence improvement and intellect enrichment by seven effective thinking patterns (SETP) tool. *International Journal of Indian Psychology*, 3 (1). DOI: 10.25215/0301.161, DIP: 18.01.161/20150301.

Stempel, H.S., Cheston, S.E., Greer, J.M., & Gillespie, C.K. (2006). Further exploration of the Vedic Personality Inventory: Validity, reliability and generalizability. *Psychological Reports*, 98, 261-273.

Tversky, A., & Kahneman, D. (1991). Loss aversion in riskless choice: A reference-dependent model. *The Quarterly Journal of Economics*, 106 (4), 1039–1061.

Usher, M., & McClelland, J. L. (2001). The time course of perceptual choice: The leaky, competing accumulator model. *Psychological Review*, 108(3), 550–592.

Usher, M., & McClelland, J. L. (2004). Loss aversion and inhibition in dynamical models of multialternative choice. *Psychological Review*, 111(3), 757–769.

Wolf, D. & Abell, N. (2003). Examining the Effects of Meditation Techniques on Psychosocial Functioning. *Research on Social Work Practice*, 13, 27-42.

Wolf, D. (1998). The Vedic Personality Inventory- A Study of the Gunas. *The Journal of Indian Psychology*, 16 (1), 26-43.

Wolf, D. (1999). A Psychometric Analysis of the Three Gunas. *Psychological Reports*, 84, 1379-1390.

Wolf, D. (1999-2). *Effects of the Hare Krsna Maha Mantra on Stress, Depression, and the Three Gunas*. Florida State University. Doctoral Dissertation.

Wolf, D. & Abell, N. (2003). Examining the Effects of Meditation Techniques on Psychosocial Functioning. *Research on Social Work Practice*, 13, 27-42.

Acknowledgements

The authors appreciate all those who participated in the study and helped to facilitate the research process.

Conflict of Interest

The authors declared no conflict of interests.

How to cite this article: M Garrido & D Wolf (2019). A mathematical model of the Gunas as a foundation for expanded understanding of decision-making process. *International Journal of Indian Psychology*, *7*(4), 466-489. DIP:18.01.056/20190704, DOI:10.25215/0704.056